Indian Journal of Engineering & Materials Sciences
Vol. 30, April 2023, pp. 283-289
DOI: 10.56042/ijems.v30i2.1370

Effect of Porosity on Hydromagnetic Boundary Layer Flow with Forced Convective Heat Transfer

K Sharma[a*], R Goyal[b], V K Joshi[c], S B Bhardwaj[d], R M Singh[e], & OD Makinde[f]

[a]Department of Mathematics, Malaviya National Institute of Technology Jaipur 302 017, India
[b]Department of Mathematics, Sanjay Ghodawat International School, Kolhapur 416 118, India
[c]Directorate of Online Education, Manipal University, Jaipur 303 007, India
[d]Department of Physics, Government College, Matak-Majri Indri, Karnal 132 041, India
[e]Department of Physics, Chaudhary Devi Lal University, Sirsa 125 055, India
[f]Faculty of Military Science, Stellenbosch University, Matieland 7602, South Africa

Received 28 April 2021; Accepted: 21 September 2021

A numerical investigation has been carried out to analyse the effect of porosity with forced convective heat transfer on steady ferrohydrodynamic (FHD) flow for water-based magnetic nanofluid over a rotating disk. The governing nonlinear coupled partial differential equations together with the boundary conditions are non-dimensionalized into a non-linear system for ordinary differential equations taking Karman's transformations. Further, the numerical solutions are obtained using the power series approximations method and presented for the velocity, temperature and skin friction profiles through graphs. For a wide range of applicability, magnetic nanofluids having Prandtl numbers ranging from 12.3 to 44.3 are taken into consideration which included well-known water-based magnetic nanofluid Taiho-W40. Also, the heat transfer rate from the disk surface, skin frictions and thickness of the boundary layer are discussed. From the results, it is noted that the rise in the porosity of Taiho-W40 enhances the flow motion in tangential as well as in axial directions. Further, there is an improvement in the heat transfer rate towards the outer environment with the increase in the Prandtl number.

Keywords: Magnetic field, Magnetic Nanofluid, Porosity, Prandtl number, Rotating Disk

1 Introduction

Magnetic nanofluids are colloidal liquids of nanoscale ferromagnetic particles synthesised in a carrier fluid. A surfactant coating is required to avoid the clogging and to enhance its life. Because of its responsive behaviour over the magnetic field, the researchers and engineers vigorously attracted for investigation on them considering the wide range of industrial applications since last six decades (Shi et al.[1], Sharma et al.[2], Philip[3]).The nano size of the spherical shaped particles enhances the heat dissipation due to increased surface area of the boundary layer. The phenomena of friction variation, heating/cooling, pressure drop, minimization of drag force, energy/mass transport etc. on nano-suspension flow become more popular among numerous researchers.

In recent decades, the rotating disk flow has become a topic of interest among several researchers due to the commonly used circular shaped devices in mechanical engineering such as crystal growth process, gas turbine systems, thermal power plants, high speed rotating machinery, etc. The thermal effect on the viscosity over a flat surface has been investigated by Vajravelu et al.[4] for flow and thermal behaviour. Das et al.[5] published the work on the time-dependent convective flow for an oscillating porous plate taking into account of thermal radiation. Ram et al.[6] investigated the convective heat transport phenomena of unsteady boundary layer flow of hydrocarbon-based nano-suspension. For understanding the radiation impacts on the magnetic nanofluid flow, a range of Prandtl number $50 \leq Pr \leq 175$ is taken by Ram et al.[7]. Chaudhary[8] applied Perturbation technique to investigate the unsteady flow of CNT-water nanofluid over a stretching plate with slip conditions. Also, many researchers[9-13] got published the results on the rotating disk problem for various nanofluid flow. Recently, Sharma et al.[14] discussed the Coriolis effect and viscous dissipation with forced convective heat transfer on steady flow of magnetic fluid considering the geometry of a rotating porous disk. Also, the impact of variable viscosity and

*Corresponding author (E-mail: maths.kushal@gmail.com)

variable conductivity on the water-based Fe_3O_4 nanofluid flow between two parallel stretchable rotating disks is discovered by Bhandari[15]. Reddy et al.[16] considered the activation energy model to investigate the transport phenomena of hybrid nanoparticle suspension in base fluid water over a rotating disk. Halawa and Tanious[17] considered Fe_3O_4-water magnetic nanofluid to numerically investigate the magnetic field arrangement for maximizing the heat exchange performance.

Porosity has been a subject of active research due to its significant importance in many fields of science and engineering like pharmaceuticals, ceramics, metallurgy, manufacturing, hydrology, earth sciences, soil mechanics etc. It is defined as a ratio of empty spaces in a material over the total volume. Porosity has a value either between 0 and 1, or as a percentage between 0% and 100%. Abbaszadeh et al.[18] considered the flow of planer channel filled with the fibrous porous medium and explained the enhancement of heat transport phenomena. The transport phenomena for heat and mass have been studied by Reddy and Chamkha[19] for a water-nano-suspension on vertical cone in the presence of porous medium. The effects of porous medium, and thermal radiation on magnetic nanofluids flow over a rotating disk are analysed by Joshi et al.[20]Moreover, Joshi et al.[21]performed a numerical investigation to study the effects of porosity on a time dependent Bodewadt flow of water-based magnetic nanofluids. Rashid and Liyang[22] discussed the impact of nano particle shape of a magnetohydrodynamic (MHD) nanofluid over a rotating stretchable disk in the presence of Darcy porous medium. Hina et al.[23] performed research on micropolar fluids for analyzing the boundary layer flow of a porous disk.

In the current study, cylindrical co-ordinates (r,θ,z)(r, θ, z) are taken into consideration to represent the modelled problem, assuming the axis of rotation as the z-axis. Here, the findings are concerned with the impact of porosity on steady flow with forced convective heat transfer of an incompressible electrically non-conducting magnetic nanofluid on a uniformly heated rotating disk in the presence of a uniform magnetic field. Moreover, the modelled equations are non-dimensionalized by appropriate similarity transformations and the resultant system is estimated the oretically using the method of power series approximations and computed numerically with help of the software MATHEMATICA 12.

In the area of fluid mechanics, rotationally symmetric flows of the incompressible magnetic nanofluids are free of the angular coordinates. Here, the investigations were performed for the water-based magnetic nanofluid. For this conducting fluid, the Prandtl numbers are taken within the range $12.3 \leq Pr \leq 44.3$. The modelled rotating disk problem of our study has several real-world engineering and industrial applications. Disk-shaped bodies are often encountered in many real-world engineering applications, and heat transfer problems of free convection boundary layer flow over a rotating disk, which occurs in rotating heat exchangers, rotating disk reactors for biofuel production, and gas or marine turbines, are extensively used by the energy, chemical, and automobile industries.

2 Materials and Methods

Here, the flow is considered through an isotropic medium to be steady and axi-symmetric. Here, the conducting magnetic nanofluid and the disk have the uniform velocity, where the magnetic-fluid and the disk, both are assumed to be electrically non-conducting. The schematic diagram for the physical model is shown in Fig. 1. The NR-model considers the magnetization $\boldsymbol{M}$(parallel to the applied magnetic field $\boldsymbol{H}$), considering Maxwell relations $\nabla \times \boldsymbol{H} = \boldsymbol{0}$, $\nabla.(\boldsymbol{H} + \boldsymbol{M}) = \boldsymbol{0}$ with assumptions $\boldsymbol{M} = \boldsymbol{\chi H}$, $\boldsymbol{M} \times \boldsymbol{H} = \boldsymbol{0}$, where, $\boldsymbol{\chi}$ is the magnetic susceptibility and is the gradient operator. The plate is maintained at constant temperature $\boldsymbol{T_w}$ and the conducting fluid stream away from the infinite disk is at $\boldsymbol{T_\infty}$. The set of governing equations (continuity equation, momentum equation and energy equation) of the unsteady axi-symmetric FHD boundary-layer flow in the cylindrical co-ordinates are given as:

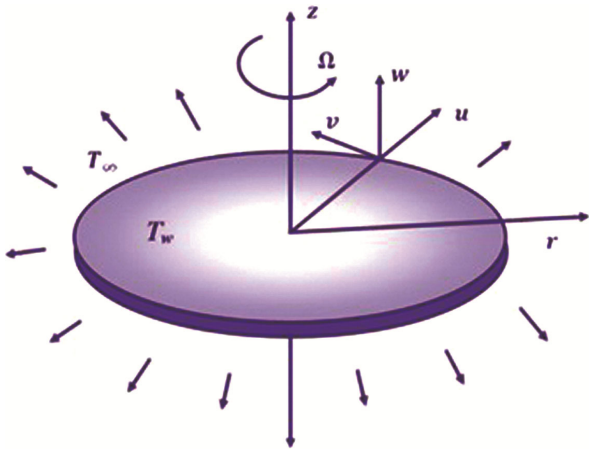

Fig. 1 — Schematic view of the physical model.

$$-\frac{1}{\rho}\frac{\partial p}{\partial r}+\frac{\mu_0}{\rho}|\boldsymbol{M}|\frac{\partial}{\partial r}|\boldsymbol{H}|+\frac{\nu}{\epsilon}\left[\frac{\partial^2 u}{\partial r^2}+\frac{\partial}{\partial r}\left(\frac{u}{r}\right)+\frac{\partial^2 u}{\partial z^2}\right]=\frac{1}{\epsilon^2}\left(u\frac{\partial u}{\partial r}+w\frac{\partial u}{\partial z}-\frac{v^2}{r}\right) \quad \ldots (1)$$

$$\nu\left[\frac{\partial^2 v}{\partial r^2}+\frac{\partial}{\partial r}\left(\frac{v}{r}\right)+\frac{\partial^2 v}{\partial z^2}\right]=\frac{1}{\epsilon}\left(u\frac{\partial v}{\partial r}+w\frac{\partial v}{\partial z}+\frac{uv}{r}\right) \quad \ldots (2)$$

$$-\frac{1}{\rho}\frac{\partial p}{\partial z}+\frac{\mu_0}{\rho}|\boldsymbol{M}|\frac{\partial}{\partial z}|\boldsymbol{H}|+\frac{\nu}{\epsilon}\left[\frac{\partial^2 w}{\partial r^2}+\frac{1}{r}\frac{\partial w}{\partial r}+\frac{\partial^2 w}{\partial z^2}\right]=\frac{1}{\epsilon^2}\left(u\frac{\partial w}{\partial r}+w\frac{\partial w}{\partial z}\right) \quad \ldots (3)$$

$$\frac{\partial u}{\partial r}+\frac{u}{r}+\frac{\partial w}{\partial z}=0 \quad \ldots (4)$$

$$\rho C_p\left(u\frac{\partial T}{\partial r}+w\frac{\partial T}{\partial z}\right)=\frac{\kappa}{\epsilon}\left(\frac{\partial^2 T}{\partial r^2}+\frac{1}{r}\frac{\partial T}{\partial r}+\frac{\partial^2 T}{\partial z^2}\right) \quad \ldots (5)$$

The approximate initial and boundary conditions for the flow are given by

$$\left.\begin{array}{l}(u,v,w)=(0,r\Omega,0),\quad p=p_0,\quad T=T_w\ \ at\ \ z=0\\(u,v,w)\to(0,0,-\beta),\quad p\to p_\infty,\ T\to T_\infty\ \ as\ \ z\to\infty\end{array}\right\} \quad \ldots (6)$$

Here, w does not disappear at $z=\infty$, but approaches to a negative value finitely. Further, to obtain the solution for the modelled system, we took the boundary layer approximation $-\frac{1}{\rho}\frac{\partial p}{\partial r}+\frac{\mu_0}{\rho}|\boldsymbol{M}|\frac{\partial}{\partial r}|\boldsymbol{H}|=-\boldsymbol{r\Omega^2}$ for Eq. (1). Only the magnetic field at the surface of the disk is considered, because the viscous boundary layer is thinner than magnetic boundary layer. So, there is no z-directional variation throughout the fluid boundary layer. By using the following similarity transformations,

$$\left.\begin{array}{l}u=r\Omega\,U(\eta),\ v=r\Omega\,V(\eta),\ w=\sqrt{\nu\Omega}\,W(\eta),\\p=\rho\Omega\nu\,P(\eta),\ T=T_\infty+(T_w-T_\infty)\theta(\eta);\text{ where }\eta=z\sqrt{\Omega/\nu}\end{array}\right\} \quad \ldots (7)$$

In the system of Eqs. (1)-(5), we found a system of coupled non-linear ordinary differential equations in $U,\ V,\ W,\ P$ and θ as follows:

$$\epsilon U''(\eta)-W(\eta)U'(\eta)-U^2(\eta)+V^2(\eta)-\epsilon^2=0 \quad \ldots (8)$$

$$\epsilon V''(\eta)-W(\eta)V'(\eta)-2U(\eta)V(\eta)=0 \quad \ldots (9)$$

$$\epsilon^2 P'(\eta)-\epsilon W''(\eta)+W(\eta)W'(\eta)=0 \quad \ldots (10)$$

$$W'(\eta)+2U(\eta)=0 \quad \ldots (11)$$

$$\theta''(\eta)-Re^2\varepsilon\,Pr\,W(\eta)\,\theta'(\eta)=0 \quad \ldots (12)$$

where, $Re=\frac{\sqrt{\nu}}{\sqrt{\Omega}\,\delta}=\text{Reynold}'\text{s number}$ and $Pr=\frac{\mu_\infty C_p}{\kappa}=\text{Prandtl number}$ and here, prime represents differentiation with respect to $'\eta'$. Also, the boundary conditions reduced to

$$\left.\begin{array}{c}U(0)=0,\ V(0)=1,\ W(0)=0,\ \theta(0)=1,\\U(\infty)=V(\infty)=0=\theta(\infty),\\W\text{ tends to a negative value finitely as}\eta\to\infty.\end{array}\right\} \quad \ldots (13)$$

The values of $U(\eta)$, $V(\eta)$, $W(\eta)$ and $\theta(\eta)$ are calculated numerically and depicted graphically for the combined effect of porosity with forced convective heat transfer. W must tend to a finite limit, say $-\beta$, as tends to infinity. However, before proceeding to the solution, attention is given briefly to the momentum equation, which may be expressed as

$$P'(\eta)=\frac{1}{\epsilon^2}\left(\epsilon W''(\eta)-W(\eta)W'(\eta)\right) \quad \ldots (14)$$

It is observed that Eq. (14) provides a relation for calculating the pressure distribution from a known axial velocity. Since the pressure distribution is somewhat secondary on the current findings, no further observation will be given to Eq. (14). For the desired solution, the formal asymptotic expansions (for large) of the Eqs (8)-(9) and Eqs (11)-(12) are the power series in $exp\,(-\beta\eta/\epsilon)$, i.e.

$$\left.\begin{array}{r}U(\eta)\approx\sum_{i=1}^{\infty}A_i e^{-i\frac{\beta\eta}{\epsilon}},\\V(\eta)\approx\sum_{i=1}^{\infty}B_i e^{-i\frac{\beta\eta}{\epsilon}},\\W(\eta)\approx W(\infty)+\sum_{i=1}^{\infty}C_i e^{-i\frac{\beta\eta}{\epsilon}},\\\theta(\eta)\approx\sum_{i=1}^{\infty}D_i e^{-i\frac{\beta\eta}{\epsilon}},\end{array}\right\} \quad \ldots (15)$$

Using the assumptions $U'(0)=a, V'(0)=b$, $\theta'(0)=-0.886\,Pr$, Eqs (8)-(9) and Eqs (11)-(12), we get the following boundary conditions to compute the approximate solution:

$$U'(0)=a, U''(0)=\frac{\epsilon^2-1}{\epsilon}, U'''(0)=\frac{-2b}{\epsilon}, U'^v(0)=\frac{-2b^2}{\epsilon}, U^v(0)=\frac{-2a\,(1+\epsilon^2)}{\epsilon} \quad \ldots (16)$$

$$V'(0)=b, V''(0)=0, V'''(0)=\frac{2a}{\epsilon}, V'^v(0)=2\left(\frac{ab}{\epsilon}-\frac{1-\epsilon^2}{\epsilon^2}\right), V^v(0)=-\frac{8b}{\epsilon^2}+4b \quad \ldots (17)$$

$$W'(0)=0, W''(0)=-2a, W'''(0)=2\left(\frac{1-\epsilon^2}{\epsilon}\right), W'^v(0)=\frac{4b}{\epsilon}, W^v(0)=\frac{4b^2}{\epsilon} \quad \ldots (18)$$

$$\left.\begin{array}{l}\theta'(0)=-0.886\,Pr,\ \theta''(0)=0,\ \theta'''(0)=0,\\\theta'^v(0)=1.772\,Re^2\epsilon\,Pr^2 a,\ \theta^v(0)=1.772\,Re^2 Pr^2(1-\epsilon^2)\end{array}\right\} \quad \ldots (19)$$

For numerical estimations of the solution, first six coefficients in the Eq. (15) for $U(\boldsymbol{\eta})$ are calculated theoretically with the help of the boundary conditions, which are as follows:

$$A_1=\left(\frac{(20\varepsilon^3-20\epsilon)c^5+45\,a\epsilon c^4-90b\epsilon^2c^2-36b^2\epsilon^2c+6a\epsilon^4(\epsilon^2+1)}{3c^5}\right),$$

$$A_2=\left(\frac{(-2540\epsilon^3+2540\epsilon)c^5-5265a\epsilon c^4+11880b\epsilon^2c^2+4860b^2\epsilon^3c-822a\varepsilon^4(\epsilon^2+1)}{180c^5}\right),$$

$$A_3=\left(\frac{(248\epsilon^3-248\epsilon)c^5+461a\epsilon c^4-1228b\epsilon^2c^2-520b^2\epsilon^3c+90a\epsilon^4(\epsilon^2+1)}{24c^5}\right),$$

$$A_4 = \left(\frac{(-242\epsilon^3 + 242\epsilon)c^5 - 411a\epsilon c^4 + 1284b\epsilon^2c^2 + 570b^2\epsilon^3c - 102a\epsilon^4(\epsilon^2+1)}{72c^5}\right),$$

$$A_5 = \left(\frac{(12\epsilon^3 - 12\epsilon)c^5 + 19a\epsilon c^4 - 68b\epsilon^2c^2 - 32b^2\epsilon^3c + 6a\epsilon^4(\epsilon^2+1)}{24c^5}\right),$$

$$A_6 = \left(\frac{\left(-\frac{2}{3}\epsilon^3 + \frac{2}{3}\epsilon\right)c^5 - a\epsilon c^4 + 4b\epsilon^2c^2 + 2b^2\epsilon^3c - \frac{2}{5}a\epsilon^4(\epsilon^2+1)}{24c^5}\right).$$

Similarly, we can find other coefficients involved in Eq. (15) for $V(\eta)$, $W(\eta)$ and $\theta(\eta)$. Further, using the values $U'(0) = a = 0.54$, $V'(0) = b = -0.62$, $\theta'(0) = -0.886\,Pr$ and $\beta = 0.886$, we calculated the numerical values of the coefficients $\{A_i,\ B_i,\ C_i,\ D_i | i = 1 \text{ to } 6,\ i \in \mathrm{N}\}$ (Table 1). We draw the graphs of velocity (radial, tangential and axial) components for distinct values of porosity, and temperature profile for different Prandtl numbers; with the dimensionless similarity parameter , taking water based magnetic nanofluid under considerations.

In the present study, the estimations of skin-friction coefficients and heat-transfer rate, which are very important through the industrial application point of view, are also calculated. The physical parameters of practical interest are the shear stress at the moving surface and the wall heat flux. Here, the radial and tangential skin-friction coefficients, and rate of heat transfer at the surface of the circular plate are also calculated. To estimate the radial stress $\boldsymbol{\tau_r}$ and the tangential shear stress $\boldsymbol{\tau_\theta}$, the Newtonian formulae can be defined using the non-dimensional variables, as

$$\tau_r = \left[\mu_\infty\left(\frac{\partial v_r}{\partial z} + \frac{\partial v_z}{\partial r}\right)\right]_{z=0} = \mu_\infty\sqrt{Re}\Omega U'(0) \text{ and } \tau_\varphi = \left[\mu_\infty\left(\frac{\partial v_\varphi}{\partial z} + \frac{1}{r}\frac{\partial v_z}{\partial \varphi}\right)\right]_{z=0} = \mu_\infty\sqrt{Re}\Omega V'(0)$$

where, $Re = r^2\Omega/\upsilon$ is the local rotational Reynolds number and hence, the radial (C_{f_r}) and azimuthal (C_{f_φ}) skin frictions are given by $Re^{\frac{1}{2}}C_{f_r} = U'(\eta)$ and $Re^{\frac{1}{2}}C_{f_\varphi} = V'(\eta)$, respectively. Also, the rate of heat transforms (Λ) from the plate surface to the ferrofluid is calculated as

$$\Lambda = -\left(\kappa\frac{\partial T}{\partial z}\right)_{z=0} = -\kappa\Delta T\left(Re^{\frac{1}{2}}\right)\theta'(0)$$

So, the Nusselt number Nu is given by $Nu = -\theta'(0)$. Here, the Table 2 represents Nusselt number for the corresponding Prandtl numbers to the conducting fluids. For the considered magnetic nanofluid flow, the boundary layer displacement thickness is also calculated using the formula:

$$d = \frac{1}{r\Omega}\int_0^\infty v\,dz = \int_0^\infty V(\eta)d\eta$$

The calculated values of boundary layer displacement thickness (d) are given in Table 3.

Table 2 — Nusselt number for various values of Prandtl number

	$Pr = 12.3$	$Pr = 28.3$	$Pr = 44.3$
$-\theta'(0)$	−10.8971798	−25.0736671	−39.2494456

Table 1 — The coefficients involve in Eq. (14)

Coefficients in the power series expansion of U(Ƞ)

ϵ	Pr	A_1	A_2	A_3	A_4	A_5	A_6
0.02	---	-0.016190	0.128800	-0.266630	0.243220	-0.108640	0.019440
0.04	---	0.151430	-0.473600	0.648020	-0.489260	0.196140	-0.032720
0.06	---	-0.041620	0.356400	-0.747730	0.684020	-0.305790	0.054720

Coefficients in the power series expansion of V(Ƞ)

ϵ	Pr	B_1	B_2	B_3	B_4	B_5	B_6
0.02	---	5.87883	-14.59315	19.41184	-14.54185	5.81265	-0.96832
0.04	---	5.75882	-14.19131	18.83225	-14.09103	5.62846	-0.93719
0.06	---	5.63995	-13.79434	18.26098	-13.64732	5.44732	-0.90659

Coefficients in the power series expansion of W(Ƞ)

ϵ	Pr	C_1	C_2	C_3	C_4	C_5	C_6
0.02	---	5.314820	-13.285969	17.714488	-13.286129	5.314684	-0.885779
0.04	---	5.311251	-13.273734	17.697692	-13.274277	5.310164	-0.885094
0.06	---	5.305239	-13.253053	17.669160	-13.254026	5.302592	-0.883910

Coefficients in the power series expansion of θ(Ƞ) at ϵ = 0.02

Re	Pr	D_1	D_2	D_3	D_4	D_5	D_6
20	12.3	14.40491	-51.952885	86.79641	-76.368052	34.37985	-6.260233
20	28.3	44.087964	-189.083376	342.434523	-315.56996	146.296032	27.165183
20	44.3	94.97224	-426.919675	788.883629	-734.982241	343.017094	-63.971046

Table 3 — Boundary-layer displacement thickness for porosity value ϵ

Porosity	$\epsilon = 0.02$	$\epsilon = 0.04$	$\epsilon = 0.06$	$\epsilon = 1$
Boundary Layer Displacement Thickness	0.0554499	0.114207	0.169599	0.734562

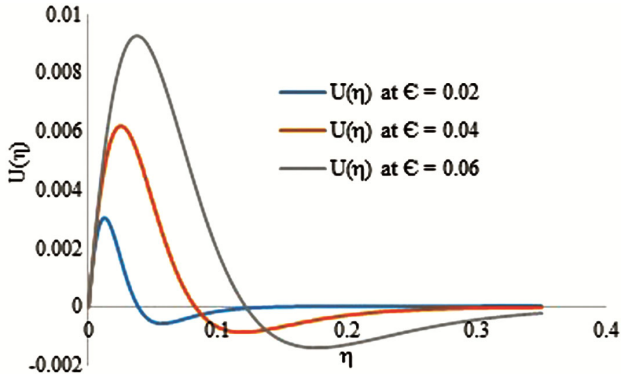

Fig. 2 — Effect of porosity on radial velocity profile.

3 Results and Discussion

In order to exhibit the influence of porosity of the water based magnetic nanofluids with forced convective heat transfer over a rotating boundary layer flow, the extensive computations for the considered flow equations are executed by the power series approximations method within the environment of the software MATHEMATICA 12. In the modelled system, Eq. (13) represents the behaviour of velocity and temperature at the boundary of the fluid flow. To perform this study, the Prandtl number ranging $12.3 \leq Pr \leq 44.3$ is taken into consideration for water based magnetic nanofluids. For the qualitative discussion, the fluid flow behaviour is presented through Figs 2–8. Also, the rate of heat transfer, and boundary layer displacement thickness; both are estimated and presented in Table 2 & Table 3, respectively.

Figures 2–4 exhibit the trends of the velocity profiles for distinct porosity values of water based magnetic nanofluids. It is observed that the radial velocity (Fig. 2) achieves its maximum values near the surface of the plate and then starts decreasing. The peak of the radial velocity enhances with the gain in the porosity. With the effect of the porosity, the radial velocity gets some negative region just before converging to the boundary condition. The behaviour of the tangential and axial velocity is shown in Figs 3–4. It is noted that both the components of velocity increase with the increase in the porosity of the fluids.

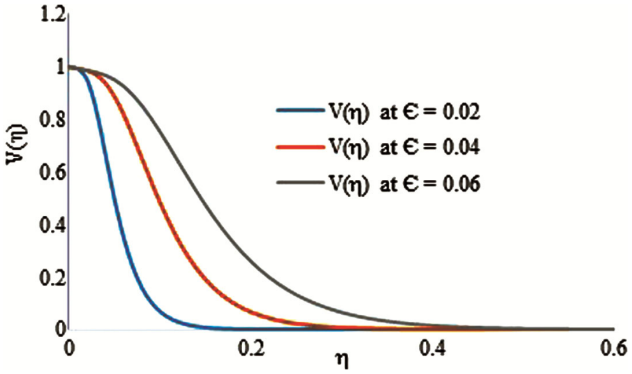

Fig. 3 — Effect of porosity on tangential velocity profile.

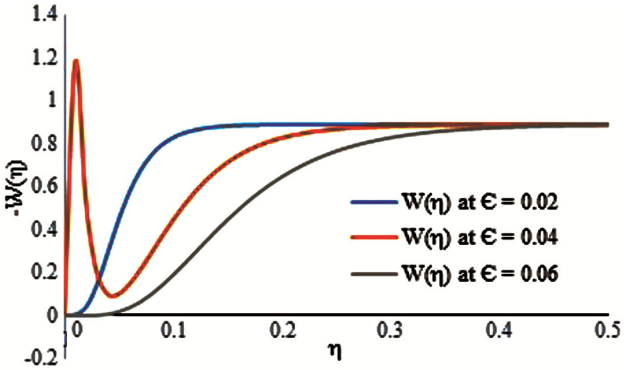

Fig. 4 — Effect of porosity on axial velocity profile.

To depict the impact of Prandtl number ($Pr = 12.3, 28.3, 44.3$) of a water based magnetic nanofluid on the temperature profile, Reynolds number 20 and 1 is considered and presented through Fig. 5 & 6, respectively. It is found that the increasing values of Prandtl number raise the temperature profile, thereby increases the thermal boundary layer thickness. Hence the heat-transfer rate drops off with the increase in Prandtl number. Also, near the surface of the plate, the rapid increase on temperature profile is observed. It is interesting to see that for Re = 20, temperature increases rapidly than at Re = 1 and have the high peak value which results the low heat dissipation in case of Re = 20.

Also, the effects of the porosity of the magnetic nanofluids on the skin friction coefficient are shown through Figs 7–8. Figure 7 shows that the radial skin-friction coefficient enhances with the gain in the porosity of the magnetic nanofluids because the viscosity of the fluids becomes higher with the increase in the porosity. In Fig. 8, the result of skin friction coefficient in the tangential direction shows an opposite behaviour as presented in Fig.7.

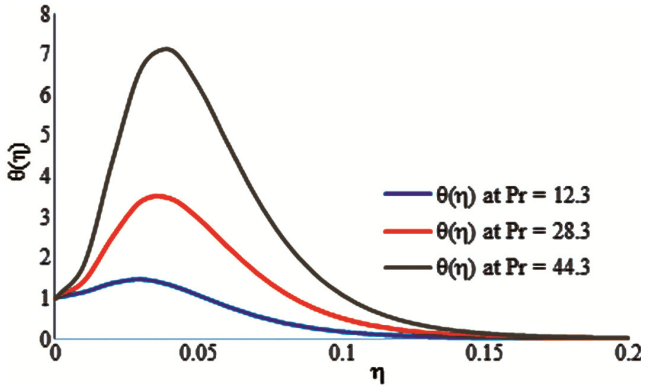

Fig. 5 — Effect of Prandtl number on temperature profile for Re = 20.

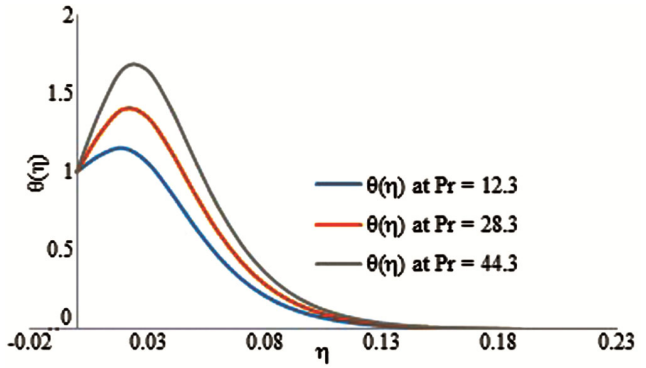

Fig. 6 — Effect of Prandtl number on temperature profile for Re = 1.

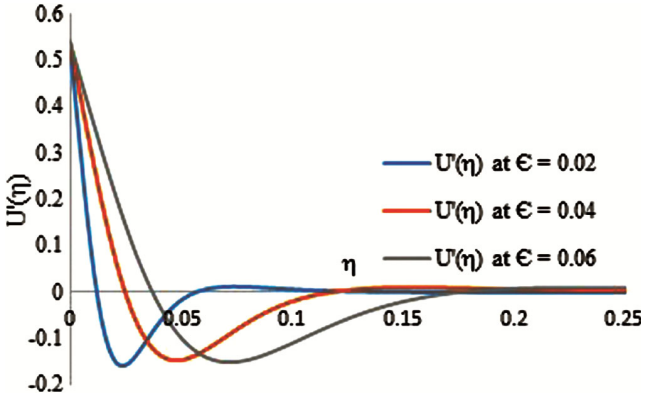

Fig. 7 — Effect of porosity on derivative of radial velocity profile.

Table 2 presents the rate of heat-transfer for varying Prandtl number and Table 3 presents the influence of porosity value on boundary layer displacement thickness of magnetic nanofluids in the boundary layer region. The negative values of Nusselt number are observed in Table 2 which is due to the heat transfer from the magnetic nanofluid to the disk surface because of increase in thermal boundary layer thickness. The heat transfer rate towards the outer environment from the nanofluid, becomes moderate with the increase in the Prandtl number. Further, the displacement thickness increases on increasing the porosity of the fluids.

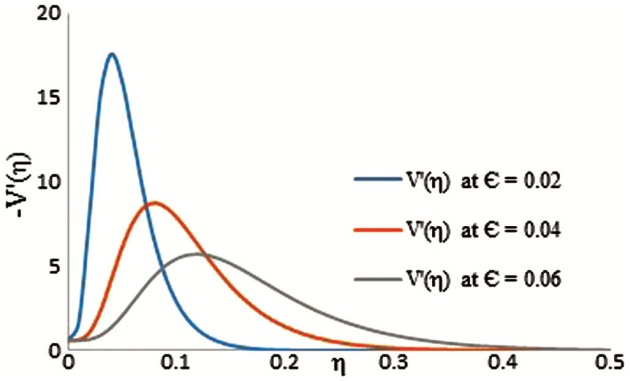

Fig. 8 — Effect of porosity on derivative of tangential velocity profile.

4 Conclusion

The main highlights of the current findings are as follows:

- Higher values of porosity of water based magnetic nanofluids increases peak value for radial velocity and it gets some negative value just before converging to its steady state.
- Rise in porosity of the nanofluids improves the fluid flow in both tangential and axial directions.
- Increasing in Prandtl number enhance temperature profiles for both case Re = 1 and Re = 20 but in case of Re = 20 temperature rises rapidly than Re = 1.
- The radial skin friction coefficient rises for increasing value of porosity of nanofluids while reverse trend is observed for tangential skin friction coefficient.

References

1 Shi L, Hu Y & He Y, *Nano Energy*, 71 (2020) 104582.
2 Sharma A K, Tiwari A K & Dixit A R, *Mater Manu Process*, 30 (2015) 813.
3 Philip J, *Adv Colloid Interface Sci*, 311 (2022) 102810.
4 Vajravelu K, Prasad K V & Ng C O, *J Hydrodyn*, 25 (2013) 1.
5 Das S, Jana R N &Makinde O D, *J Mech,* 32 (2016) 197.
6 Ram P, Joshi V K &Makinde O D, *Defect Diffus*, 377 (2017) 155.
7 Ram P, Joshi V K, Sharma S, & Yadav N, *Mater Sci Forum*,928 (2018) 100.
8 Chaudhary S, *Indian J Eng Mater Sci,* 27 (2020) 396.
9 Ram P & Sharma K, *Indian J Pure Appl Phys*, 52 (2014) 87.
10 Shehzad S A, Mabood F, Rauf A &Tlili I, *Int Commun Heat Mass Transf*, 116 (2020) 104693.
11 Bhandari A, *Proc. Inst. Mech. Eng. Part C J Mech Eng Sci*, 235 (2021) 2201.

12 Sharma K, Vijay N, Kumar S & Makinde O D, *Heat Transfer*, 50 (2021) 4342.
13 Sharma K, *Pramana - J Phys*, 95 (2021) 113.
14 Sharma K, Vijay N, Makinde O D, Bhardwaj S B, Singh R M, & Mabood F, *Chaos, Soliton Fract*, 148 (2021) 111055.
15 Bhandari A, *Int. J. Appl. Comput. Math*, 7 (2021) 46.
16 Reddy M G, Kumar N, Prasannakumara B C, Rudraswamy N G & Kumar K G, *CommunTheor Phys*, 73 (2021) 045002.
17 Halawa T &Tanious A S, *Int J Therm Sci*, 184 (2023) 108014.
18 Abbaszadeh M, Salehi A &Abbassi A, *J porous media*, 20 (2017) 175.
19 Reddy P S &Chamkha A J, *J porous Media*, 20 (2017) 1.
20 Joshi V K, Ram P, Tripathi D & Sharma K, *Thermal Science,* 22 (2018) 2883.
21 Joshi V K, Ram P, Sharma R K & Tripathi D, *Eur Phys J Plus*, 132 (2017) 1.
22 Rashid U & Liang H,*Int J Numer Methods Heat Fluid Flow*, 30 (2020) 5169.
23 Hina S, Roman U, Inam S, Kanwal S & Bilal M, *P I Mech Eng E-J Pro*, 236(2022) 2147.